

# Nickel(II) complexes chelated by 2-quinoxaliny-6-iminopyridines: Synthesis, crystal structures and ethylene oligomerization

Sherrif Adewuyi <sup>a</sup>, Gang Li <sup>a,b</sup>, Shu Zhang <sup>a</sup>, Wenqing Wang <sup>a</sup>, Peng Hao <sup>a</sup>,  
Wen-Hua Sun <sup>a,\*</sup>, Ning Tang <sup>b</sup>, Jianjun Yi <sup>c</sup>

<sup>a</sup> Key Laboratory of Engineering Plastics and Beijing National Laboratory for Molecular Sciences, Institute of Chemistry, Chinese Academy of Sciences, Beijing 100080, China

<sup>b</sup> State Key Laboratory of Applied Organic Chemistry, Lanzhou University, Lanzhou 730000, China

<sup>c</sup> Petrochemical Research Institute, PetroChina Company Limited, No. 20 Xueyuan Road, Beijing 100083, China

Received 1 February 2007; received in revised form 20 April 2007; accepted 24 April 2007

Available online 1 May 2007

## Abstract

A series of nickel(II) complexes ligated by tridentate ligands of 2-quinoxaliny-6-iminopyridines was synthesized and characterized by elemental and spectroscopic analysis as well X-ray diffraction analysis. X-ray crystallographic analysis revealed the nickel complexes as five-coordinated distorted trigonal bipyramidal geometry. In the presence of Et<sub>2</sub>AlCl, these complexes displayed high catalytic activity for ethylene oligomerization and the dimmers were produced as main products. The nickel dibromide complexes exhibited relative higher activity than their dichloride analogues. Both elevation of the ethylene pressure and addition of auxiliary ligand have catalytic enhancement effects on all the complexes.

© 2007 Elsevier B.V. All rights reserved.

**Keywords:** Nickel complexes; 2-Quinoxaliny-6-iminopyridines; Ethylene oligomerization

## 1. Introduction

The selection of metal–ligand combinations suitable as catalyst for ethylene oligomerization and/or polymerization has been at the heart of the discovery process and one of the most noteworthy advances in this regard has been the increased prominence of late transition metal systems. After the pioneering work of Keim that formed the basis of SHOP process [1]; the interest resurgence period of Brookhart group (1995) that culminated diimine Ni-catalyst system [2], many research efforts have centered on four coordinated nickel (II) complexes bearing bidentate ligands. Some examples in this regard include: diimine [3]; imino-pyridine [4]; imino-phenol [5]; salicylaldimine

[5,6]; 8-iminoquinoline [7] and anilinetropine [8] ligands. More importantly, as a follow up to independent discovery of bis(arylimino)pyridyl Fe(II) and Co(II) dihalides by Brookhart [9] and Gibson [10], the zeal for designing five-coordinated nickel(II) dihalides has been on the rise. By careful modification of the ligand backbones, Ni(II) complexes bearing tridentate chelates of P<sup>^</sup>N<sup>^</sup>N [11] and N<sup>^</sup>N<sup>^</sup>N [12] models have been developed. Remarkably, the ethylene oligomerization productivities of these models varied from moderate to high.

In exploring new catalyst for ethylene oligomerization in our laboratory with tridentate chelated model, nickel (II) complexes were designed and investigated for their catalytic performance bearing ligands such as carboxylate ester substituted monoiminopyridine (O<sup>^</sup>N<sup>^</sup>N) [13], diphenylphosphinoanilines (P<sup>^</sup>N<sup>^</sup>P) [14], diarylphosphinoquinoline-8-amines (P<sup>^</sup>N<sup>^</sup>N) [14], 2,9-bis(imino)-1,10-phenanthroline (N<sup>^</sup>N<sup>^</sup>N) [15], 2-imino-1,10-phenanthroline

\* Corresponding author.

E-mail address: [whsun@iccas.ac.cn](mailto:whsun@iccas.ac.cn) (W.-H. Sun).

(N<sup>^</sup>N<sup>^</sup>N) [16] and 2-benzimidazolylpyridines (N<sup>^</sup>N<sup>^</sup>N) [17]. All these catalysts exhibited considerably good to high activity for ethylene oligomerization upon activation either with MAO and/or Et<sub>2</sub>AlCl. In furtherance of our research in this field, synthesis and ethylene reactivity study of new metal halides bearing 2-quinoxalanyl-6-iminopyridine analogues with various *ortho*-positioned substituents on the aryl ring is being embarked upon. Their iron complexes gave good catalytic activities for ethylene reactivity (oligomerization and polymerization) upon activation with methylaluminoxane (MAO), while their cobalt analogues showed moderate activities toward ethylene oligomerization with modified methylaluminoxane (MMAO) [18]. Successively, the nickel analogues were synthesized and characterized. Owing to the large  $\pi$ -system present in the ligand backbone, this is proposed to increase the Lewis-acidity of the coordinated nickel center by strong ability to accommodate negative charge. The net effect is the stabilization of the catalyst active center and consequently, rendering a positive impact on the catalytic activity. Herein, we report the synthesis, molecular structures and ethylene oligomerization capability of Ni(II) complexes containing monoiminopyridine-quinoxalanyl extended ligands.

## 2. Results and discussion

### 2.1. Synthesis and characterization

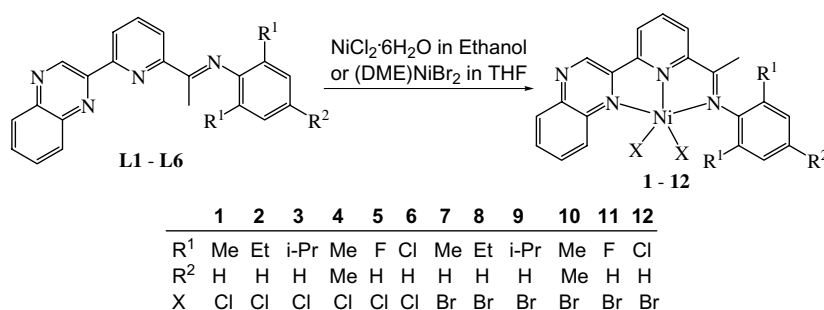
The compounds used as ligands **L1–L6** were efficiently synthesized according to our reported procedure [18]. The dichloride nickel complexes (**1–6**) were synthesized by reactions of NiCl<sub>2</sub> · 6H<sub>2</sub>O with the ligands **L1–L6** in ethanol (Scheme 1). The mixture of NiCl<sub>2</sub> · 6H<sub>2</sub>O with the corresponding ligand was stirred at room temperature for 12 h, the resulting solution was concentrated and diethyl ether was thereafter added to precipitate the product. The precipitate was collected, washed several times with diethyl ether and dried in vacuum. Meanwhile the dibromide nickel complexes (**9–12**) were synthesized through the reaction of ligands **L1–L6** with (DME) NiBr<sub>2</sub> in THF under nitrogen atmosphere. All of these complexes were formed by this method in excellent yields, and their structures were confirmed by IR spectra and elemental analysis. The IR

spectra of the ligands show that the C=N stretching frequencies of the ligands appear in the range 1638–1646 cm<sup>-1</sup> with strong intensities, however, in the complexes (**1–12**), the C=N stretching frequencies shifted toward lower values, between 1606 and 1631 cm<sup>-1</sup> with weak intensities. The results reveal the coordination interaction between the imino nitrogen atom and the nickel center. In addition, the unambiguous molecular structures of complexes **1**, **3**, **8**, **9** and **12** were confirmed by the single-crystal X-ray diffraction studies.

### 2.2. Molecular structures

Crystals of complexes **1**, **3**, **8**, **9** and **12** suitable for X-ray structural determination were obtained by crystallization through the slow diffusion of diethyl ether into their dichloromethane solution. Analysis of X-ray crystallography reveals that all complexes are five-coordinated with the geometry of distorted trigonal bipyramidal. Their selected bond lengths and angles are collected in Table 1.

In the solid state of **1** (Fig. 1), the pyridyl nitrogen atom and two chlorine atoms form the equatorial plane with the equatorial plane angles range between 102.23(1)° and 129.15(8)°. The two axial Ni–N bonds subtend an angle of 155.51(2)°, a distortion that is a consequence of satisfying the tridentate chelating constrains of the ligand. The axial plane is oriented almost orthogonally (ca. 89.4°) to the equatorial plane. All the atoms of pyridine ring and the N3, C14 of the imino group as well as N1, C8 of the quinoxalanyl group make an almost perfect plane with the mean deviation of 0.0457 Å and the nickel atom lie 0.1397 Å out of this plane. The dimethylphenyl ring is oriented almost orthogonally (82.7°) to this plane. The two axial Ni–N bond lengths, 2.144(4) Å and 2.163(4) Å are longer than that of the pyridyl nitrogen atom (1.965(4) Å), a geometry similar to that observed in the 2-imino-1,10-Phenanthroline nickel complexes [16]. There is a significant difference in the two Ni–Cl linkages, the Cl1 being about 0.081 Å shorter than that of Cl2, which could be attributed to the bipyramidal geometry where the longer Ni–Cl bond was associated with the apical site. There is no evidence of any bond delocalization involving the imines, the C=N bond having typical double-bond character (1.283(6) Å). In the solid state, complex **1** dis-



Scheme 1. Synthesis of the nickel complexes **1–12**.

Table 1  
Selected bond lengths (Å) and angles (°) for **1**, **3**, **8**, **9** and **12**

	<b>1</b>	<b>3</b>	<b>8</b>	<b>9</b>	<b>12</b>
<i>Bond lengths</i>					
Ni–N(1)	2.144(4)	2.186(3)	2.219(4)	2.199(4)	2.141(4)
Ni–N(2)	1.965(4)	1.978(3)	1.983(4)	1.975(4)	1.968(4)
Ni–N(3)	2.163(4)	2.157(3)	2.150(5)	2.172(4)	2.191(4)
Ni–X(1)	2.2206(2)	2.2802(1)	2.3675(1)	2.4255(9)	2.3746(8)
Ni–X(2)	2.3014(2)	2.2427(9)	2.3996(1)	2.3733(9)	2.4142(8)
N(3)–C(14)	1.283(6)	1.281(4)	1.272(7)	1.283(7)	1.289(6)
<i>Bond angles</i>					
N(1)–Ni–N(2)	78.55(2)	77.40(1)	76.88(2)	77.33(2)	78.74(2)
N(1)–Ni–N(3)	155.51(2)	154.55(1)	153.42(2)	154.53(2)	155.15(4)
N(2)–Ni–N(3)	77.20(2)	77.53(1)	76.99(2)	77.71(2)	76.59(2)
N(1)–Ni–X(1)	92.84(1)	86.35(8)	102.42(1)	85.91(1)	96.82(1)
N(1)–Ni–X(2)	90.44(1)	99.55(8)	90.20(1)	99.76(1)	90.27(1)
N(2)–Ni–X(1)	128.13(1)	99.09(8)	147.68(1)	98.11(1)	130.78(1)
N(2)–Ni–X(2)	102.23(1)	136.63(8)	100.50(1)	137.76(1)	99.81(1)
N(3)–Ni–X(1)	99.36(1)	101.87(8)	97.06(1)	102.60(1)	96.97(1)
N(3)–Ni–X(2)	98.00(1)	95.63(8)	99.22(1)	95.26(1)	96.78(1)
X(1)–Ni–X(2)	129.15(8)	124.08(4)	111.83(4)	123.91(4)	129.36(3)

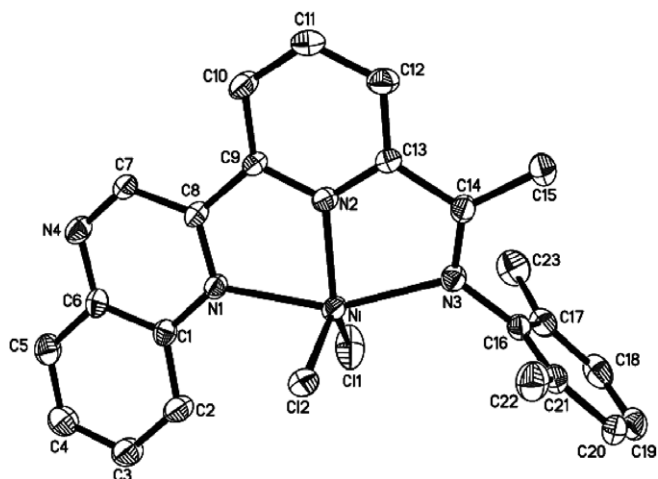


Fig. 1. Molecular structure of complex **1** with thermal ellipsoids at the 30% probability level. Hydrogen atoms have been omitted for clarity.

Table 2  
Hydrogen-bond interactions for complex **1**

D–H...A	D–H	H...A	D...A	∠DHA (°)
C7–H7A...Cl2	0.930	2.682	3.605	171.85
C10–H10A...Cl2	0.930	2.806	3.697	160.68
C15–H15A...N4	0.960	2.586	3.472	153.58

plays intermolecular hydrogen bonding interactions (Fig. 2 and Table 2). As a consequence of these hydrogen bonding interactions, this complex exhibits a 2D supramolecular structure via C–H...Cl and C–H...N hydrogen bonds along the  $[1,0,1]$  and  $[-1,0,1]$  directions, respectively (Fig. 2).

As shown in Fig. 3, the geometry in complex **3** is similar with that in complex **2**. The pyridyl nitrogen atom and two chlorine atoms form the equatorial plane while the axial

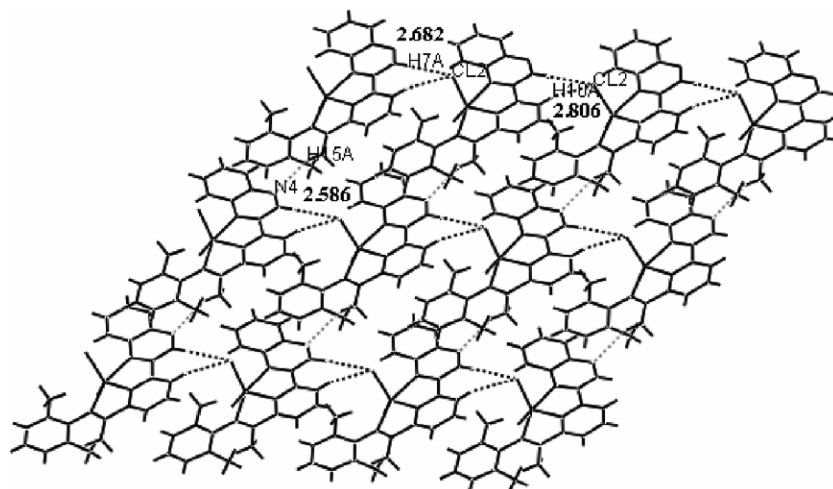


Fig. 2. The 2-D chain formed by intermolecular hydrogen bonding interactions in complex **1**.

plane includes the other two nitrogen atoms and the nickel center. The nickel atom is almost coplanar with the equatorial plane with the deviation of 0.0532 Å. The equatorial angles are 99.09(8)°, 124.08(4)° and 136.63(8)°, respectively, which showed great difference with that in complex **1**. The difference could be attributed to the different substituent at the *ortho*-position of the phenyl ring. The axial Ni–N bonds form a N1–Ni–N3 angle of 154.55(1). Similar with complex **1**, the two axial Ni–N bond lengths, 2.186(3) Å and 2.157(3) Å are longer than that of the pyridyl nitrogen atom (1.978(3) Å). The equatorial plane and the phenyl ring on the imino-C are nearly perpendicular to the pyridine plane with the dihedral angles of 93.4° and 99.1° respectively. The two Ni–Cl bond distances show a difference of 0.037 Å, which is much smaller than the aryl methyl-substituted complex **1**. In complex **3**, hydrogen bonds between two neighboring molecules linked them to 1-D infinite polymer chain. In addition, the solvent molec-

ular dichloromethane attach to the polymer chain by hydrogen bond (Fig. 4).

The nickel dibromide complex **8** (Fig. 5) with 2,6-diethylphenyl and complex **9** (Fig. 7) with 2,6-diisopropyl almost have the same structural characters. One nitrogen atom of the pyridyl group and two chlorides form the equatorial plane, while the nickel atom lies 0.0024 and 0.0569 Å out of the equatorial plane in **8** and **9**, respectively. Due to the different substituent on the phenyl ring, these two complexes show different equatorial angles. The equatorial angles are 100.50(1)°, 111.83(4)° and 147.68(1)° for **8** and 98.11(1)°, 123.91(4)° and 137.76(1)° for **9**. The equatorial planes of these two complexes are nearly orthogonal to the pyridyl plane, with dihedral angles of 92.0° in **8** and 93.4° in **9**. The dihedral angle between the phenyl plane on the imino-N group and the pyridyl plane is 88.7° in **8**, which is much smaller than that in **9** (100.2°). Similar to the nickel dichloride analogues, the Ni–N bonds in the

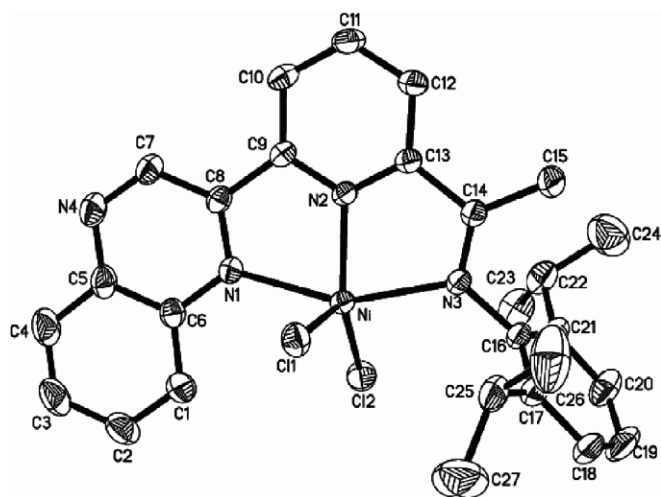


Fig. 3. Molecular structure of complex **3** with thermal ellipsoids at the 30% probability level. Hydrogen atoms and solvent have been omitted for clarity.

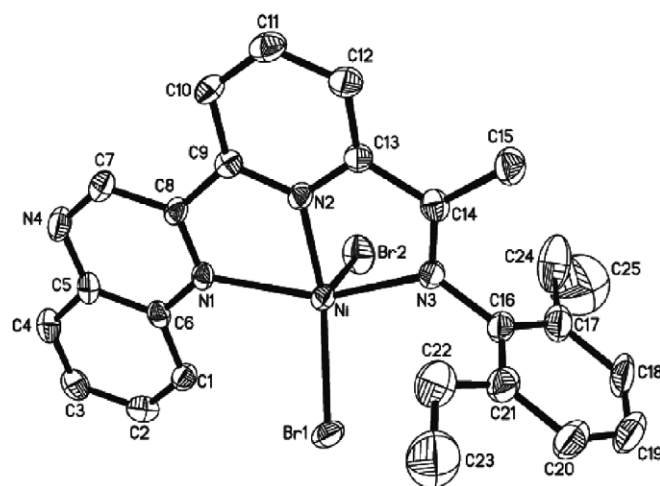


Fig. 5. Molecular structure of complex **8** with thermal ellipsoids at the 30% probability level. Hydrogen atoms have been omitted for clarity.

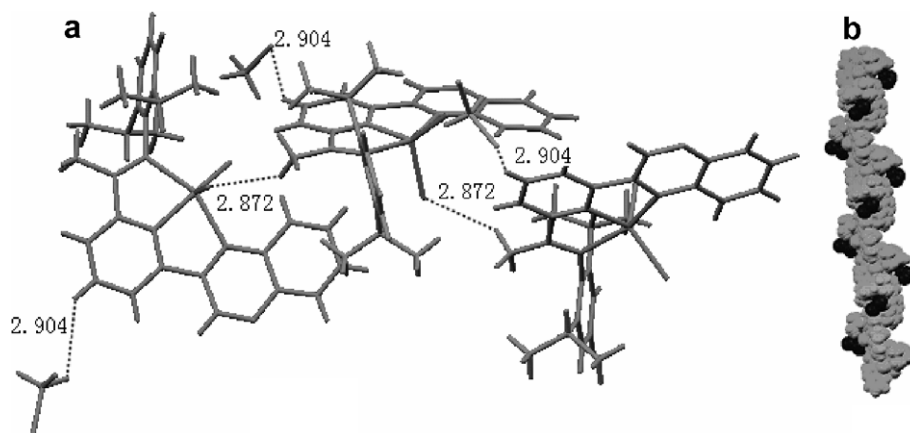


Fig. 4. (a) The 1-D chain formed by intermolecular hydrogen bonding interactions (C11...H15B) in complex **3**. (b) The spacefill structure of the polymer chain (the black ones are dichloromethane molecules).

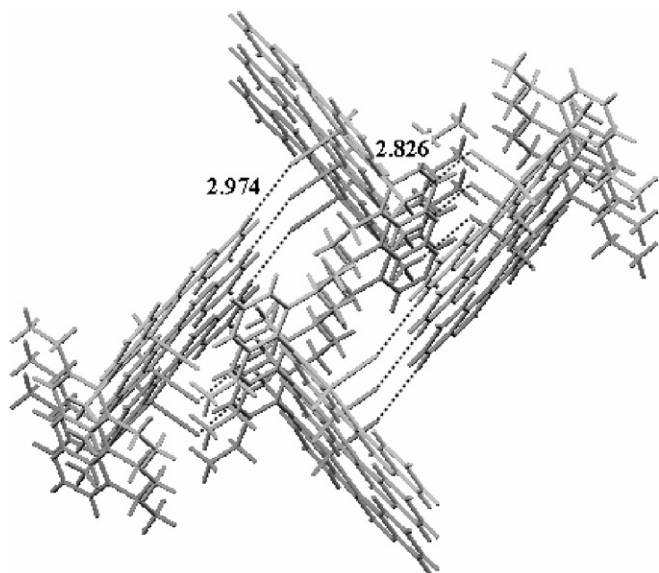


Fig. 6. A view of the crystal packing for complex **8**.

equatorial plane are longer than that in the axial plane. The difference in bond distance is about 0.03 Å in **8** and 0.05 Å in **9**. The two imino C=N bonds have distinctive double-bond character, with C–N distance of 1.272(7) Å (**8**) and 1.283(7) Å (**9**). Comparing nickel dibromide complex **9** with dichloride **3** bearing the same ligand, no obvious influence on the molecular geometry was observed. This conclusion is based on the similar bond lengths and angles of these two complexes. In the solid state, complex **8** displays intermolecular hydrogen bonding interactions. The hydrogen bond C10–H10A···Br1 (2.982 Å) linked different molecules together to form a 1-D infinite chain. In addition, as shown in Fig. 6, four chains were nest together by two different kinds of hydrogen bond: C15–H15B···Br2 (2.826 Å) and C4–H4B···Br2 (2.974 Å).

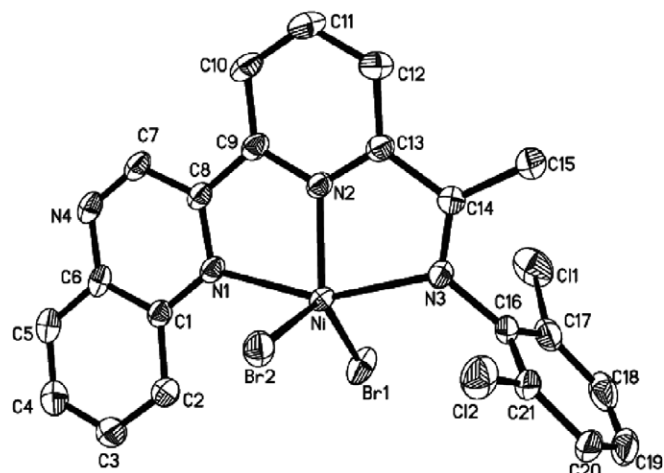


Fig. 8. Molecular structure of complex **12** with thermal ellipsoids at the 30% probability level. Hydrogen atoms and isolated water molecules have been omitted for clarity.

As shown in Fig. 8, in the solid state of complex **12** with 2,6-dichlorophenyl, the nitrogen atom of pyridyl and two bromides form the equatorial plane with the nickel atom slightly deviating by 0.0274 Å from this plane. The three equatorial angles are respectively 99.81(1)°, 130.78(1)° and 129.36(3)°, with a larger Br–Ni–Br angle than its 2,6-dialkylphenyl analogues, while the axial N1–Ni–N3 angles is 155.15(4)°. Both the equatorial plane and the phenyl plane link to imino-N are almost perpendicular to the pyridyl plane, with the dihedral angles of 90.6° and 84.1°, respectively. Similar to its analogues, the two axial Ni–N bond lengths, 2.141(4) Å and 2.191(4) Å, are longer than that of Ni–N2 in the equatorial plane 1.968(4) Å. Furthermore, the two Ni–Br show a difference of about 0.04 Å. The imino C14–N3 bond has typical C=N double-bond character, with a bond length of 1.289(6) Å, which is slightly longer than that of the analogues with 2,6-dialkylphenyl substituents.

### 2.3. Ethylene oligomerization

#### 2.3.1. The selection of co-catalyst

Initial scanning of trimethylaluminum (Me<sub>3</sub>Al), methylaluminumoxane (MAO) and its modified form (MMAO) as activators of the titled Ni(II) complexes for ethylene oligomerization at ambient pressure of ethylene yielded low activities in the order of  $-10^4$  g mol<sup>-1</sup> (Ni) h<sup>-1</sup>. However, a comparable response was obtained from the catalyst activator, diethylaluminumchloride (Et<sub>2</sub>AlCl), with improved oligomerization activity of  $5.7 \times 10^4$  g mol<sup>-1</sup> (Ni) h<sup>-1</sup>. The catalysts productivities further improved at elevated ethylene pressure. The 1/Et<sub>2</sub>AlCl system showed higher catalytic activity than the other systems activated with MAO and Me<sub>3</sub>Al (entries 2, 4 and 5, Table 3). Therefore, further investigations were carried out at elevated ethylene pressure and Et<sub>2</sub>AlCl as the choice co-catalyst. The obtained results are presented in Table 3.

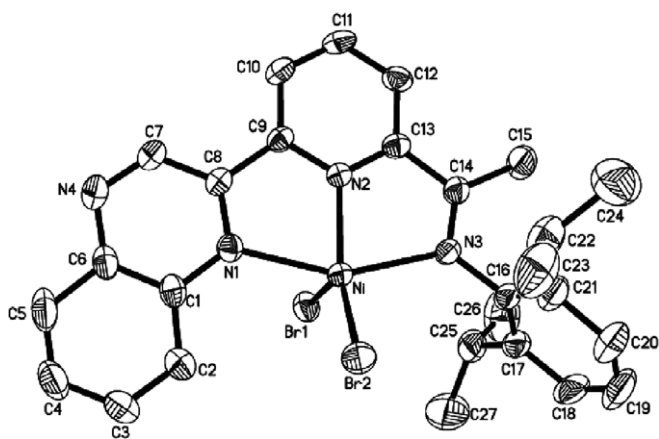


Fig. 7. Molecular structure of complex **9** with thermal ellipsoids at the 30% probability level. Hydrogen atoms and isolated water molecules have been omitted for clarity.

Table 3  
Ethylene oligomerization with complexes **1–12**/Et<sub>2</sub>AlCl<sup>a</sup>

Entry	Complex	Al/Ni	P (atm)	T (°C)	Activity (10 <sup>5</sup> g mol <sup>-1</sup> (Ni) h <sup>-1</sup> )	Oligomers distribution (%)	
						C <sub>4</sub>	C <sub>6</sub>
1	<b>1</b>	500	10	20	2.1	94.2	5.8
2	<b>1</b>	700	10	20	6.9	96.7	3.3
3	<b>1</b>	1000	10	20	3.5	>99	
4 <sup>b</sup>	<b>1</b>	700	10	20	3.8	100	
5 <sup>c</sup>	<b>1</b>	700	10	20	0.4	100	
6 <sup>d</sup>	<b>1</b>	700	10	20	3.7	99.2	0.8
7 <sup>e</sup>	<b>1</b>	700	10	20	9.7	98.3	1.7
8	<b>1</b>	700	20	20	7.9	87.7	12.3
9	<b>1</b>	700	30	20	13.7	61.8	38.2
10	<b>1</b>	700	10	30	1.6	97.5	2.5
11	<b>1</b>	700	10	40	1.4	97.0	3.0
12	<b>2</b>	700	10	20	6.1	89.6	10.4
13	<b>3</b>	700	10	20	5.3	85.9	14.1
14	<b>4</b>	700	10	20	5.0	92.1	7.9
15	<b>5</b>	700	10	20	1.1	99.1	0.9
16	<b>6</b>	700	10	20	5.6	97.7	2.3
17	<b>7</b>	700	10	20	7.4	84.2	15.8
18	<b>7</b>	700	20	20	8.5	87.5	12.5
19	<b>7</b>	700	30	20	18.6	97.6	2.4
20	<b>8</b>	700	10	20	6.3	89.1	10.9
21	<b>9</b>	700	10	20	5.2	97.4	3.6
22	<b>10</b>	700	10	20	2.2	77.7	22.3
23	<b>11</b>	700	10	20	2.3	98.5	1.5
24	<b>12</b>	700	10	20	5.9	97.8	2.2

<sup>a</sup> General conditions: 5 μmol cat.; 100 mL toluene as solvent; 30 min.

<sup>b</sup> Cocat: MAO.

<sup>c</sup> Cocat: Me<sub>3</sub>Al.

<sup>d</sup> Solvent: heptane (100 mL).

<sup>e</sup> Solvent: dichloromethane (100 mL).

### 2.3.2. Effect of reaction parameters

As depicted in Table 3, the reaction parameters including the ratio of Et<sub>2</sub>AlCl to nickel complex, reaction temperature and ethylene pressure grossly affected their catalytic performances. The influences of the Al/Ni molar ratio and the reaction temperature were investigated in detail with complex **1**. The results indicate a high influence of varied Al/Ni ratio on the oligomerization activity. The catalytic activity reached optimum value of 6.9 × 10<sup>5</sup> g mol<sup>-1</sup> (Ni) h<sup>-1</sup> with the ratio of 700. Subsequently, the activity sharply dropped and the value of 3.5 × 10<sup>5</sup> g mol<sup>-1</sup> (Ni) h<sup>-1</sup> was obtained with the Al/Ni ratio of 1000 (Entries 1–3, Table 3). A similar trend was observed in our previous work [16]. As initially proposed, a possible reason could be that a threshold amount of Et<sub>2</sub>AlCl as co-catalyst was needed to efficiently activate the catalyst precursor, but, large amount might cause such deactivation [19].

Changing the solvent by using the heptane (Entry 6, Table 3), lower activity of ethylene oligomerization was observed. However, when the dichloromethane was used as solvent for ethylene oligomerization, relative higher activity was obtained. But from the GC chart, some new compounds were observed, which could be attributed the reaction of dichloromethane and Et<sub>2</sub>AlCl. In this case, fur-

ther investigations were carried out using toluene as solvent.

Apparently, the ethylene concentration significantly affects the catalytic behavior of the complexes. The catalytic systems **1**/Et<sub>2</sub>AlCl and **7**/Et<sub>2</sub>AlCl were investigated under different ethylene pressure. The activities of these complexes rose sharply with increasing ethylene pressure and at 30 atmospheres, values of 1.37 and 1.86 × 10<sup>6</sup> g mol<sup>-1</sup> (Ni) h<sup>-1</sup> were obtained respectively (Entries 9 and 19, Table 3). Variation of the reaction temperature also affects the catalytic performance with little or no influence on the distribution of low-order C<sub>4</sub> and C<sub>6</sub> oligomers produced (Entries 2, 10 and 11, Table 3). Complex **1** displayed higher oligomerization activity at lower temperature and at elevated temperatures of 30 °C while at 40 °C, a significant reduction in activity was observed compared with that at 20 °C. The prominent reason might be unfavorable active sites and lower ethylene solubility at higher temperature.

### 2.3.3. Effect of the ligand environments

The dependence of catalytic activities of all the complexes [(L)NiCl<sub>2</sub> (**1–6**) and (L)NiBr<sub>2</sub> (**7–12**)] on halide anion linkage to the nickel center was monitored. In most cases, the nickel dibromide precursors showed better activity than their corresponding dichloride precursors. This observation is in concord with the reported pyrazolyliminophosphorane based Ni(II) analogue [11b] and the effect is attributable to higher solubility of the dibromides in the toluene solvent medium than the dichlorides counterparts. In addition, with the increased ethylene pressure, the nickel dichloride **1** produced more trimers (Entries 2, 8–9, Table 3). However, the opposite trend was observed for the nickel dibromide **7** (Entries 17–19, Table 3). A noticeable effect of the alkyl substituents on the aryl ring of the complexes is also worth mentioning. For the nickel dichloride complexes, a reduction of steric bulk at the *ortho*-aryl position resulted in increase activity of the complexes. Hence, complexes **1** with methyl groups in the *ortho*-positions of the aryl ring showed better activities of 6.9 × 10<sup>5</sup> g mol<sup>-1</sup> (Ni) h<sup>-1</sup> at 10 atmospheres ethylene. The introduction of substituent at the *para*-position of the phenyl group resulted in decreased activity (Entry 14, Table 3). Complex **6**, which bear 2,6-dichlorophenyl group showed comparable catalytic activity than its analogues bearing 2,6-dialkylphenyl groups. However, complex **5**, which contain 2,6-difluorophenyl group, showed relative lower activity. The nickel dibromide complexes followed the same trend as the nickel dichloride complexes.

### 2.3.4. Effect of the auxiliary ligand on catalyst activity

The application of triphenylphosphine (PPh<sub>3</sub>) as an auxiliary ligand with nickel-based catalyst for ethylene oligomerization has proved worth while due to the high enhancement of the catalyst activity [13,15,19]. In order to examine this effect on the quinoxalin-based iminopyridine nickel halides, ethylene oligomerization with all the titled complexes was carried out in the presence of 10

Table 4  
Ethylene oligomerization with complexes **1–12**/Et<sub>2</sub>AlCl and 10 equiv of PPh<sub>3</sub>

Entry	Complex	P (atm)	Activity (10 <sup>5</sup> g mol <sup>-1</sup> (Ni) h <sup>-1</sup> )	Oligomers distribution (%)	
				C <sub>4</sub>	C <sub>6</sub>
1	<b>1</b>	1	7.2	96.8	3.2
2	<b>2</b>	1	5.9	97.1	2.9
3	<b>3</b>	1	2.3	85.0	15.0
4	<b>4</b>	1	1.3	97.7	2.3
5	<b>5</b>	1	2.4	98.6	1.4
6	<b>6</b>	1	1.5	94.6	5.4
7	<b>7</b>	1	8.5	96.2	3.8
8	<b>8</b>	1	6.1	97.6	2.4
9	<b>9</b>	1	2.0	82.7	17.3
10	<b>10</b>	1	4.8	97.0	3.0
11	<b>11</b>	1	3.4	97.1	2.9
12	<b>12</b>	1	2.2	98.7	1.3
13 <sup>b</sup>	<b>1</b>	10	10.4	95.2	4.8
14 <sup>b</sup>	<b>7</b>	10	12.0	95.6	4.4

<sup>a</sup> General conditions: 5 μmol catalyst; Al/Ni = 700; 30 mL toluene as solvent; reaction temperature: 20 °C; 30 min.

<sup>b</sup> 100 mL toluene as solvent.

equivalent amount of PPh<sub>3</sub>. As shown in Table 4, the catalytic activities of the complexes were much more improved at ambient ethylene pressure, in which, a low performance in the order of  $-10^4$  g mol<sup>-1</sup> (Ni) h<sup>-1</sup> was initially recorded. Also, complexes **5** and **9** with the best catalytic performance at 10 atmosphere ethylene, behaved in a similar manner in the presence of PPh<sub>3</sub> at ambient ethylene pressure with activities of 7.2 and  $8.5 \times 10^5$  g mol<sup>-1</sup> (Ni) h<sup>-1</sup> respectively (Entries 1 and 7, Table 4). The oligomerization products of the complexes as in the case without PPh<sub>3</sub> are mainly low-order carbon number oligomers (C<sub>4</sub> and C<sub>6</sub>) with high preference for C<sub>4</sub>. Increasing ethylene pressure to 10 atmospheres, complexes **5** and **9** further gave improved activities of 1.04 and  $1.2 \times 10^6$  g mol<sup>-1</sup> (Ni) h<sup>-1</sup> respectively in the presence of PPh<sub>3</sub> auxiliary ligand (Entries 13 and 14, Table 4). The plausible explanation, so far, offered for the activity enhancement role of PPh<sub>3</sub> is simultaneous association and dissociation with nickel metal core and consequent activation and protection of the active sites [15]. We are presently embarking on further research to unravel the mechanistic details of this effect.

### 3. Conclusion

The synthesis and characterization of new Ni(II) halides complexes with asymmetrical 2-quinoxaliny-6-iminopyridine ligands have been successfully achieved. Upon activation with Et<sub>2</sub>AlCl, all the complexes reveal moderate to good catalytic activity for the dimerization and trimerization of ethylene at low temperature and 10 atmospheres ethylene. Due to higher solubility of the nickel bromide precursors in toluene solvent medium, their catalytic performance for ethylene oligomerization are slightly higher than the corresponding nickel chloride precursors. Both elevation of the ethylene pressure and addition of auxiliary

ligand have catalytic enhancement effects on all the complexes.

## 4. Experimental

### 4.1. General considerations

All manipulations of air and/or moisture sensitive compounds were performed under nitrogen atmosphere using standard Schlenk techniques. Solvents were dried by the appropriate drying reagents and distilled under nitrogen prior to use. Et<sub>2</sub>AlCl (1.90 mol l<sup>-1</sup>) solution in hexane was purchased from Acros Chemicals. All other reagents were purchased from Aldrich and were directly used without further purification unless otherwise stated. IR spectra were recorded on a Perkin–Elmer system 2000 FT-IR spectrometer. Elemental analysis was performed on a Flash EA 1112 microanalyser. GC analyses were performed with a VARIAN CP-3800 gas chromatograph equipped with a flame ionization detector and a 30 m (0.2 mm i.d., 0.25 μm film thickness) CP-Sil 5 CB column. The yield of oligomers was calculated by referencing with the mass of the solvent based on the prerequisite that the mass of each fraction is approximately proportional to its integrated areas in the GC trace.

### 4.2. Synthesis of LNiX<sub>2</sub> (1–12; X = Cl or Br)

The complexes **1–12** were synthesized by the reaction of NiCl<sub>2</sub> · 6H<sub>2</sub>O in ethanol or (DME)NiBr<sub>2</sub> in THF with the corresponding ligands. A typical synthetic procedure for complex **1** is described as the following. The ligand **L1** (0.070 g, 0.2 mmol) and NiCl<sub>2</sub> · 6H<sub>2</sub>O (0.047 g, 0.2 mmol) was added to a Schlenk tube together with 10 ml of freshly distilled ethanol. The reaction mixture was then stirred for 12 h at room temperature after which the solvent volume was reduced to 4 ml. Absolute diethyl ether (10 ml) was added to precipitate the complex and the mixture was allowed to stand for 30 min. The supernatant was removed and the precipitate was washed with diethyl ether twice and dried in vacuum to obtain a brownish powder in 93.0% (0.09 g) yield. IR (KBr, cm<sup>-1</sup>): 1621 (w, ν<sub>C=N</sub>), 1589, 1375, 1215, 759, 744, 417. Anal. Calc. (C<sub>23</sub>H<sub>20</sub>Cl<sub>2</sub>NiN<sub>4</sub>): N, 11.62; C, 57.31; H, 4.18. Found: N, 11.37; C, 56.90; H, 4.10%. Data of complex **2** are as follow: Yield: 84.9% (0.085 g), IR (KBr, cm<sup>-1</sup>): 1609 (w, ν<sub>C=N</sub>), 1591, 1480, 1445, 1375, 1276, 1129, 1095, 818, 774, 415. Anal. Calc. (C<sub>25</sub>H<sub>24</sub>Cl<sub>2</sub>NiN<sub>4</sub>): N, 10.98; C, 58.87; H, 4.74. Found: N, 11.01; C, 59.10; H, 4.83%. Data of complex **3** are as follow: Yield: 87.6% (0.094 g), IR (KBr, cm<sup>-1</sup>): 1606 (w, ν<sub>C=N</sub>), 1590, 1541, 1458, 1373, 1265, 1208, 1095, 810. Anal. Calc. (C<sub>27</sub>H<sub>28</sub>Cl<sub>2</sub>NiN<sub>4</sub>): N, 10.41; C, 60.26; H, 5.24. Found: N, 10.52; C, 59.82; H, 5.26%. Data of complex **4** are as follow: Yield: 96.3% (0.099 g), IR (KBr, cm<sup>-1</sup>): 1614 (w, ν<sub>C=N</sub>), 1593, 1484, 1370, 1219, 1095, 816, 775, 418. Anal. Calc. (C<sub>24</sub>H<sub>22</sub>Cl<sub>2</sub>NiN<sub>4</sub>): N, 11.29; C, 58.11; H, 4.47. Found: N, 11.57; C, 57.86; H, 4.23%. Data of complex **5** are as follow:

Yield: 62.0% (0.06 g), IR (KBr,  $\text{cm}^{-1}$ ): 1624 (w,  $\nu_{\text{C}=\text{N}}$ ), 1593, 1483, 1426, 1370, 1262, 1225, 1096, 803, 405. Anal. Calc. ( $\text{C}_{21}\text{H}_{14}\text{Cl}_2\text{F}_2\text{NiN}_4$ ): N, 11.44; C, 51.48; H, 2.88. Found: N, 11.56; C, 51.74; H, 3.11%. Data of complex **6** are as follow: Yield: 67.0% (0.07 g), IR (KBr,  $\text{cm}^{-1}$ ): 1625 (w,  $\nu_{\text{C}=\text{N}}$ ), 1590, 1480, 1436, 1371, 1262, 1095, 1028, 803, 405. Anal. Calc. ( $\text{C}_{21}\text{H}_{14}\text{Cl}_4\text{NiN}_4$ ): N, 10.72; C, 48.24; H, 2.70. Found: N, 10.88; C, 47.96; H, 2.54%. Data of complex **7** are as follow: Yield: 96.4% (0.110 g), IR (KBr,  $\text{cm}^{-1}$ ): 1626 (w,  $\nu_{\text{C}=\text{N}}$ ), 1590, 1479, 1373, 1211, 1097, 773, 417. Anal. Calc. ( $\text{C}_{23}\text{H}_{20}\text{Br}_2\text{NiN}_4$ ): N, 9.81; C, 48.39; H, 3.53. Found: N, 9.56; C, 48.14; H, 3.55%. Data of complex **8** are as follow: Yield: 89.0% (0.106 g), IR (KBr,  $\text{cm}^{-1}$ ): 1631 (w,  $\nu_{\text{C}=\text{N}}$ ), 1583, 1436, 1257, 1082, 852, 709, 396. Anal. Calc. ( $\text{C}_{25}\text{H}_{24}\text{Br}_2\text{NiN}_4$ ): N, 9.35; C, 50.13; H, 4.04. Found: N, 10.10; C, 49.91; H, 4.01%. Data of complex **9** are as follow: Yield: 92.8% (0.125 g), IR (KBr,  $\text{cm}^{-1}$ ): 1614 (w,  $\nu_{\text{C}=\text{N}}$ ), 1592, 1502, 1482, 1371, 1277, 1212, 1093, 817, 772, 417. Anal. Calc. ( $\text{C}_{27}\text{H}_{28}\text{Br}_2\text{NiN}_4$ ): N, 8.94; C, 51.72; H, 4.50. Found: N, 8.12; C, 52.30; H, 5.08%. Data of complex **10** are as follow: Yield: 97.0% (0.130 g), IR (KBr,  $\text{cm}^{-1}$ ): 1618 (w,  $\nu_{\text{C}=\text{N}}$ ), 1593, 1503, 1484, 1370, 1277, 1219, 1095, 816, 775, 418. Anal. Calc. ( $\text{C}_{24}\text{H}_{22}\text{Br}_2\text{NiN}_4$ ): N, 9.58; C, 49.28; H, 3.79. Found: N, 9.26; C, 50.10; H, 3.53%. Data of complex **11**

are as follow: Yield: 62.0% (0.06 g), IR (KBr,  $\text{cm}^{-1}$ ): 1624 (w,  $\nu_{\text{C}=\text{N}}$ ), 1593, 1483, 1426, 1370, 1262, 1225, 1096, 803, 405. Anal. Calc. ( $\text{C}_{21}\text{H}_{14}\text{Cl}_2\text{F}_2\text{NiN}_4$ ): N, 11.44; C, 51.48; H, 2.88. Found: N, 11.56; C, 51.74; H, 3.11%. Data of complex **12** are as follow: Yield: 79.5% (0.10 g), IR (KBr,  $\text{cm}^{-1}$ ): 1619 (w,  $\nu_{\text{C}=\text{N}}$ ), 1591, 1471, 1372, 1280, 1226, 1076, 776, 580. Anal. Calc. ( $\text{C}_{21}\text{H}_{14}\text{Cl}_2\text{Br}_2\text{NiN}_4$ ): N, 9.16; C, 41.23; H, 2.31. Found: N, 9.01; C, 40.71; H, 2.42%.

#### 4.3. Procedure for ethylene oligomerization

Ethylene oligomerization at 1 atm of ethylene was carried out as follows: Complex (5  $\mu\text{mol}$ ) was added to a Schlenk flask under nitrogen. The flask was back-filled three times with  $\text{N}_2$  and twice with ethylene and thereafter charged with toluene and co-catalyst solutions in turn under ethylene atmosphere. The reaction solution was vigorously stirred under 1 atm of ethylene at the set temperature. At the end of the desired period of time, the reaction was quenched by 5% aqueous hydrogen chloride and the products were analyzed by GC.

The oligomerization at higher ethylene pressure was performed in a 0.25 L stainless steel autoclave equipped with mechanical stirrer, a temperature controller and gas ballast through a solenoid valve for continuous feeding of ethylene

Table 5  
Crystal data and structure refinement for compounds **1**, **3**, **8**, **9** and **12**

Data	<b>1</b>	<b>3</b> · $\text{CH}_2\text{Cl}_2$	<b>8</b>	<b>9</b> · $2\text{H}_2\text{O}$	<b>12</b> · $3\text{H}_2\text{O}$
Formula	$\text{C}_{23}\text{H}_{20}\text{Cl}_2\text{N}_4\text{Ni}$	$\text{C}_{28}\text{H}_{30}\text{Cl}_4\text{N}_4\text{Ni}$	$\text{C}_{25}\text{H}_{24}\text{Br}_2\text{N}_4\text{Ni}$	$\text{C}_{27}\text{H}_{28}\text{Br}_2\text{N}_4\text{Ni} \cdot \text{O}_2$	$\text{C}_{21}\text{H}_{14}\text{Br}_2\text{Cl}_2\text{N}_4\text{NiO}_3$
Fw	482.04	623.07	599.01	659.06	659.79
Color	Brown	Brown	Brown	Brown	Brown
Temperature (K)	293(2)	293(2)	293(2)	293(2)	293(2)
Crystal system	Orthorhombic	Rhombohedral	Monoclinic	Rhombohedral	Monoclinic
Space group	<i>Fdd2</i>	<i>R-3</i>	<i>P2(1)/c</i>	<i>R-3</i>	<i>P2(1)/n</i>
<i>a</i> (Å)	31.1073(7)	26.7441(3)	9.6064(19)	27.0801(6)	8.80010(1)
<i>b</i> (Å)	32.1295(9)	26.7441(3)	14.944(3)	27.0801(6)	18.4102(3)
<i>c</i> (Å)	8.6723(2)	22.7376(6)	17.090(3)	23.1749(1)	16.3100(3)
$\beta$ (°)	90	90	98.22(3)	90	104.2220(1)
<i>V</i> (Å <sup>3</sup> )	8667.6(4)	14084.2(4)	2428.1(8)	14718.0(8)	2561.42(7)
<i>Z</i>	16	18	4	18	4
Wavelength (Å)	0.71073	0.71073	0.71073	0.71073	0.71073
<i>D</i> <sub>calc</sub> (mg m <sup>-3</sup> )	1.478	1.322	1.639	1.338	1.711
Crystal size (mm)	0.32 × 0.23 × 0.16	0.35 × 0.25 × 0.20	0.40 × 0.30 × 0.30	0.40 × 0.30 × 0.30	0.30 × 0.20 × 0.20
$\theta$ Range (°)	1.82–28.27	1.52–28.28	1.82–25.01	1.50–28.32	1.70–28.33
Limiting indices	−41 ≤ <i>h</i> ≤ 33, −37 ≤ <i>k</i> ≤ 41, −11 ≤ <i>l</i> ≤ 11	−35 ≤ <i>h</i> ≤ 35, −35 ≤ <i>k</i> ≤ 35, −26 ≤ <i>l</i> ≤ 29	−11 ≤ <i>h</i> ≤ 11, 0 ≤ <i>k</i> ≤ 17, 0 ≤ <i>l</i> ≤ 20	−35 ≤ <i>h</i> ≤ 36, −36 ≤ <i>k</i> ≤ 36, −29 ≤ <i>l</i> ≤ 30	−11 ≤ <i>h</i> ≤ 11, −24 ≤ <i>k</i> ≤ 24, −21 ≤ <i>l</i> ≤ 15
Reflections collected/unique	11990/5133	68949/7712	8360/4244	66303/8104	24529/6344
<i>R</i> (int)	0.0457	0.0231	0.0401	0.0562	0.0323
Data/restraints/parameters	5133/1/271	7712/0/334	4244/0/284	8104/0/325	6344/18/299
Absorption coefficient (mm <sup>-1</sup> )	1.160	0.984	4.110	3.063	4.115
<i>F</i> (000)	3968	5796	1200	5976	1296
Final <i>R</i> indices	<i>R</i> <sub>1</sub> = 0.0573, [ <i>I</i> ] > 2σ( <i>I</i> ) <i>wR</i> <sub>2</sub> = 0.1377	<i>R</i> <sub>1</sub> = 0.0656, <i>wR</i> <sub>2</sub> = 0.2174	<i>R</i> <sub>1</sub> = 0.0589, <i>wR</i> <sub>2</sub> = 0.1217	<i>R</i> <sub>1</sub> = 0.0639, <i>wR</i> <sub>2</sub> = 0.2224	<i>R</i> <sub>1</sub> = 0.0509, <i>wR</i> <sub>2</sub> = 0.1704
<i>R</i> indices (all data)	<i>R</i> <sub>1</sub> = 0.0852, <i>wR</i> <sub>2</sub> = 0.1484	<i>R</i> <sub>1</sub> = 0.0787, <i>wR</i> <sub>2</sub> = 0.2342	<i>R</i> <sub>1</sub> = 0.0841, <i>wR</i> <sub>2</sub> = 0.1323	<i>R</i> <sub>1</sub> = 0.1160, <i>wR</i> <sub>2</sub> = 0.2612	<i>R</i> <sub>1</sub> = 0.0735, <i>wR</i> <sub>2</sub> = 0.1863
Goodness of fit	1.099	1.076	1.051	1.063	1.056
Largest difference in peak and hole (e Å <sup>-3</sup> )	0.621 and −0.422	1.762 and −1.295	0.693 and −0.408	1.756 and −0.804	1.604 and −0.629

at desired pressure. 100 ml of toluene containing the catalyst precursor was transferred to the fully dried reactor under nitrogen atmosphere. The required amount of  $\text{Et}_2\text{AlCl}$  was then injected into the reactor using a syringe. At the prescribed temperature, the reactor was pressurized to corresponding ethylene pressure and mechanically stirred for 30 min. The reaction was subsequently quenched and products were analyzed employing same method as described above with 1 atm ethylene.

#### 4.4. X-ray Crystal structural determination of **1**, **3**, **8**, **9** and **12**

Intensity data for complexes **1**, **3**, **9** and **12** were collected on a Bruker SMART 1000 CCD diffractometer with graphite-monochromated Mo  $K\alpha$  radiation ( $\lambda = 0.71073 \text{ \AA}$ ). Single-crystal X-ray diffraction studies for complex **8** were carried out on a Rigaku RAXIS Rapid IP diffractometer with graphite-monochromated Mo  $K\alpha$  radiation ( $\lambda = 0.71073 \text{ \AA}$ ). Unit cell dimensions were obtained with least-squares refinements. Intensities were corrected for Lorentz and polarization effects and empirical absorption. The structures were solved by direct methods, and refined by full-matrix least-square on  $F^2$ . Each hydrogen atom was placed in a calculated position, and refined using a riding model. All non-hydrogen atoms were refined anisotropically. Structure solution and refinement were performed using SHELXL-97 package [20]. Crystal data and processing parameters were summarized in Table 5.

#### Acknowledgements

This work was supported by NSFC No. 20674089 and MOST 2006AA03Z553. S.A is grateful to the Chinese Academy of Science (CAS) and The Academy of Science for The Developing World (TWAS) for the Postgraduate Fellowships.

#### Appendix A. Supplementary material

CCDC 639011, 639012, 639013, 639014 and 639015 contain the supplementary crystallographic data for **1**, **3**, **8**, **9** and **12**. These data can be obtained free of charge via <http://www.ccdc.cam.ac.uk/conts/retrieving.html>, or from the Cambridge Crystallographic Data Centre, 12 Union Road, Cambridge CB2 1EZ, UK; fax: (+44) 1223-336-033; or e-mail: [deposit@ccdc.cam.ac.uk](mailto:deposit@ccdc.cam.ac.uk). Supplementary data associated with this article can be found, in the online version, at [doi:10.1016/j.jorganchem.2007.04.036](https://doi.org/10.1016/j.jorganchem.2007.04.036).

#### References

- [1] (a) W. Keim, F.H. Kowaldt, R. Goddard, C. Krüger, *Angew. Chem., Int. Ed. Engl.* 17 (1978) 466;  
 (b) W. Keim, B. Hoffmann, R. Lodewick, M. Peuckert, G. Schmitt, *J. Mol. Catal. A: Chem.* 6 (1979) 79;

- (c) W. Keim, A. Behr, B. Limbäcker, C. Krüger, *Angew. Chem., Int. Ed. Engl.* 22 (1983) 503;  
 (d) W. Keim, A. Behr, G. Kraus, *J. Organomet. Chem.* 251 (1983) 377;  
 (e) W. Keim, *Angew. Chem., Int. Ed. Engl.* 29 (1990) 235.
- [2] (a) L.K. Johnson, C.M. Killan, M. Brookhart, *J. Am. Chem. Soc.* 117 (1995) 6414;  
 (b) C.M. Killan, L.K. Johnson, M. Brookhart, *Organometallics* 16 (1997) 2005.
- [3] (a) J. Feldman, S.J. McLain, A. Parthasarathy, W.J. Marshall, J.C. Calabrese, S.D. Arthur, *Organometallics* 16 (1997) 1514;  
 (b) M. Helldörfer, J. Backhaus, W. Milius, H.G. Alt, *J. Mol. Catal. A: Chem.* 193 (2003) 59;  
 (c) D.H. Camacho, E.V. Ziller, J.W. Ziller, Z. Guann, *Angew. Chem., Int. Ed. Engl.* 43 (2004) 1821.
- [4] (a) T.V. Laine, M. Klinga, M. Leskela, *Eur. J. Inorg. Chem.* (1999) 959;  
 (b) T.V. Laine, K. Lappalainen, J. Liimatta, E. Aitola, B. Lofgren, M. Leskela, *Macromol. Rapid Commun.* 20 (1999) 487;  
 (c) T.V. Laine, U. Piironen, K. Lappalainen, M. Klinga, E. Aitola, M. Leskela, *J. Organomet. Chem.* 606 (2000) 112;  
 (d) S.P. Meneghetti, P.J. Lutz, J. Kress, *Organometallics* 18 (1999) 2734;  
 (e) A. Koppl, H.G. Alt, *J. Mol. Catal. A: Chem.* 154 (2000) 45;  
 (f) S. Jie, D. Zhang, T. Zhang, W.-H. Sun, J. Chen, Q. Ren, D. Liu, G. Zheng, W. Chen, *J. Organomet. Chem.* 690 (2005) 1739.
- [5] L. Wang, W.-H. Sun, L. Han, Z. Li, Y. Hu, C. He, C. Yan, *J. Organomet. Chem.* 650 (2002) 59.
- [6] (a) C. Wang, S. Friedrich, T.R. Younkin, R.T. Li, R.H. Grubbs, D.A. Bansleben, M.W. Day, *Organometallics* 17 (1998) 3149;  
 (b) T.R. Younkin, E.F. Connor, J.I. Henderson, S.K. Friedrich, R.H. Grubbs, D. A Bansleben, *Science* 287 (2000) 460.
- [7] Z. Li, W.-H. Sun, Z. Ma, Y. Hu, C. Shao, *Chin. Chem. Lett.* 12 (2001) 691.
- [8] F.A. Hicks, M. Brookhart, *Organometallics* 20 (2001) 3217.
- [9] (a) B.L. Small, M. Brookhart, A.M.A. Bennett, *J. Am. Chem. Soc.* 120 (1998) 4049;  
 (b) B.L. Small, M. Brookhart, *J. Am. Chem. Soc.* 120 (1998) 7143.
- [10] (a) G.J.P. Britovsek, V.C. Gibson, S.J. McTavish, G.A. Solan, A.J.P. White, D.J. Williams, B.S. Kimberley, P.J. Maddox, *Chem. Commun.* (1998) 849;  
 (b) G.J.P. Britovsek, M. Bruce, V.C. Gibson, B.S. Kimberley, P.J. Maddox, S. Mastroianni, S.J. McTavish, C. Redshaw, G.A. Solan, S. Strömberg, A.J.P. White, D.J. Williams, *J. Am. Chem. Soc.* 121 (1999) 8728;  
 (c) G.J.P. Britovsek, S. Mastroianni, G.A. Solan, S.P.D. Baugh, C. Redshaw, V.C. Gibson, A.J.P. White, D.J. Williams, M.R.J. Elsegood, *Chem. Eur. J.* 6 (2000) 2221.
- [11] (a) F. Speiser, P. Braunstein, L. Saussine, *Dalton Trans.* (2004) 1539;  
 (b) C. Zhang, W.-H. Sun, Z.-X. Wang, *Eur. J. Inorg. Chem.* (2006) 4895.
- [12] (a) S. Al-Benna, M.J. Sarsfield, M. Thornton-Pert, D.L. Ormsby, P.J. Maddox, P. Breš, M. Bochmann, *J. Chem. Soc., Dalton Trans.* (2000) 4247;  
 (b) F.A. Kunrath, R.F. Souza, O.L. Casagrande Jr., N.R. Brooks, V.J. Yzz Jr., *Organometallics* 22 (2003) 4739;  
 (c) R. Santi, A.M. Romano, A. Somazzi, M. Grande, C. Bianchini, G. Mantovani, *J. Mol. Catal. A: Chem.* 229 (2005) 191;  
 (d) N. Ajellal, M.C.A. Kuhn, A.D.F. Boff, M. Hörner, C.M. Thomas, J.-F. Carpentier, O.L. Casagrande, *Organometallics* 25 (2006) 1213.
- [13] (a) X. Tang, W.-H. Sun, T. Gao, J. Hou, J. Chen, W. Chen, *J. Organomet. Chem.* 690 (2005) 1570;  
 (b) W.-H. Sun, X. Tang, T. Gao, B. Wu, W. Zhang, H. Ma, *Organometallics* 23 (2004) 5037;  
 (c) W. Zhang, W.-H. Sun, B. Wu, S. Zhang, H. Ma, Y. Li, J. Chen, P. Hao, *J. Organomet. Chem.* 691 (2006) 4759.
- [14] J. Hou, W.-H. Sun, S. Zhang, H. Ma, Y. Deng, X. Lu, *Organometallics* 25 (2006) 236.

- [15] L. Wang, W.-H. Sun, L. Han, H. Yang, Y. Hu, X. Jin, J. Organomet. Chem. 658 (2002) 62.
- [16] (a) W.-H. Sun, S. Zhang, S. Jie, W. Zhang, Y. Li, H. Ma, J. Chen, K. Wedeking, R. Fröhlich, J. Organomet. Chem. 691 (2006) 4196;  
(b) W.-H. Sun, S. Jie, S. Zhang, W. Zhang, Y. Song, H. Ma, J. Chen, K. Wedeking, R. Fröhlich, Organometallics 25 (2006) 666;  
(c) S. Jie, S. Zhang, K. Wedeking, W. Zhang, H. Ma, X. Lu, Y. Deng, W.-H. Sun, C.R. Chim. 9 (2006) 1500.
- [17] (a) P. Hao, S. Zhang, W.-H. Sun, Q. Shi, S. Adewuyi, X. Lu, P. Li, Organometallics 26 (2007) 2439;  
(b) W.-H. Sun, P. Hao, S. Zhang, Q. Shi, W. Zuo, X. Tang, X. Lu, Organometallics 26 (2007) 2720.
- [18] W.-H. Sun, P. Hao, G. Li, S. Zhang, W. Wang, J. Yi, M. Asma, N. Tang, J. Organomet. Chem., in press, doi:10.1016/j.jorganchem.2007.04.027.
- [19] (a) S. Mecking, Angew. Chem., Int. Ed. 40 (2001) 534;  
(b) C. Shao, W.-H. Sun, Z. Li, Y. Hu, L. Han, Catal. Comm. 3 (2002) 405.
- [20] G.M. Sheldrick, SHELXTL-97, Program for the Refinement of Crystal Structures, University of Gottingen, Germany, 1997.